Sequential eIF5 binding to the charged disordered segments of eIF4G and eIF2β stabilizes the 48S pre-initiation complex and promotes its shift to the initiation mode

Chingakham Ranjit Singh, Ryosuke Watanabe, Wasimul Chowdhury, Hiroyuki Hiraishi, Marcelo J. Murai, Yasufumi Yamamoto, David Miles, Yuka Ikeda, Masayo Asano, and Katsura Asano

Published Version Information

Citation: Singh, C. R., Watanabe, R., Chowdhury, W., Hiraishi, H., Murai, M. J., Yamamoto, Y., . . . Asano, K. (2012). Sequential eukaryotic translation initiation factor 5 (eIF5) binding to the charged disordered segments of eIF4G and eIF2β stabilizes the 48S preinitiation complex and promotes its shift to the initiation mode. Molecular and Cellular Biology, 32(19), 3978-3989.

Digital Object Identifier (DOI): doi:10.1128/MCB.00376-12

Publisher's Link: http://mcb.asm.org/content/32/19/3978.full

Sequential eIF5 binding to the charged disordered segments of eIF4G and eIF2β stabilizes the 48S pre-initiation complex and promotes its shift to the initiation mode

Chingakham Ranjit Singh, Ryosuke Watanabe, Wasimul Chowdhury, Hiroyuki Hiraishi, Marcelo J. Murai, Yasufumi Yamamoto, David Miles, Yuka Ikeda, Masayo Asano, and Katsura Asano#

Molecular Cellular and Developmental Biology Program, Division of Biology, Kansas State University, Manhattan, KS 66506, USA

#Corresponding author: Katsura Asano, kasano@ksu.edu

Running title: eIF4G RS1 domain modulates eIF1 release

Abstract

During translation initiation in *Saccharomyces cerevisiae*, an Arg- and Ser-rich segment (RS1 domain) of eIF4G and the Lys-rich segment (K-boxes) of eIF2β bind three common partners, eIF5, eIF1 and mRNA. Here we report that both of these segments are involved in mRNA recruitment and AUG recognition by distinct mechanisms. First, the eIF4G-RS1 interaction with eIF5-C-terminal domain (CTD) directly links eIF4G to the pre-initiation complex (PIC) and enhances mRNA binding. Second, eIF2β-K-boxes increase mRNA binding to the 40S subunit *in vitro*, in a manner reversed by eIF5-CTD. Third, mutations altering eIF4G-RS1, eIF2β-K-boxes and eIF5-CTD restore the accuracy of start codon selection impaired by a eIF2β mutation *in vivo*, suggesting that the mutual interactions of the eIF segments within the PIC prime the ribosome for initiation in response to start codon selection. We propose that the rearrangement of interactions involving eIF5-CTD promotes mRNA recruitment through mRNA binding by eIF4G and eIF2β and assists the start-codon-induced release of eIF1, the major antagonist of establishing $tRNA_i^{Met}$:mRNA binding to the P-site.

Introduction

In eukaryotic translation, initiation factors (eIFs) promote dissociation of vacant 80S (canonical initiation) or post-termination (recycling) ribosomes and assist binding of Met-$tRNA_i^{Met}$ and 5'-capped mRNA to the 40S subunit to form 43S and 48S pre-initiation complexes (PICs), respectively (for reviews, see (15, 17)). eIF2 binds Met-$tRNA_i^{Met}$ dependent on GTP bound to its γ subunit, delivering it to the 40S subunit. The 43S complex additionally contains eIF1A, eIF1, eIF3 and eIF5, the latter three forming a multifactor complex (MFC) with the eIF2/GTP/Met-$tRNA_i^{Met}$ ternary complex (TC) (3, 40). Except for eIF3, which binds the solvent side of the 40S subunit (39), these factors bind the decoding site of the 40S subunit, and together play a role in positioning Met-$tRNA_i^{Met}$ in the P-site. The cytoplasmic mRNA cap-binding complex eIF4F is made of three subunits, the major scaffold eIF4G, m^7G-cap-binding subunit eIF4E, and the mRNA helicase, eIF4A. eIF4F primes the 5`-proximal area of the $m^7$G-capped mRNA by the action of eIF4A, and recruits the 43S complex to the primed region of the mRNA to form the 48S PIC. According to the scanning model, the 5`-proximal 48S complex migrates downstream along the mRNA, searching for the start codon.

Currently, much effort is devoted to understanding the mechanism by which these initiation factors coordinately regulate the state of the 48S PIC. During scanning, the PIC is presumed to be in the scanning-competent "open" state, and once a start codon is reached, it is shifted to the "closed" state, establishing $tRNA_i^{Met}$:mRNA binding in the P-site. Thus, the PIC in the closed state does not scan; instead it tightly binds the selected start codon, in order to promote formation of the 40S initiation complex (IC) (6, 22). eIF1 is present in the PIC in the open state and plays a major role in antagonizing stable

$tRNA_i^{Met}$:mRNA binding to the P-site, thus suppressing transition to the closed state (28, 31). The release of eIF1 in response to AUG selection is considered to be the key regulatory event during the ribosome response to a start codon (10). eIF5 promotes GTP hydrolysis of eIF2-GTP upon or subsequent to the PIC formation (GTPase activation protein or GAP function), but the GDP and inorganic phosphate resulting from the hydrolysis remain bound to eIF2. Inorganic phosphate is released after eIF1 release, allowing eIF2-GDP to be ejected from the ribosome (2).

While eIF1 release is considered primarily as a ribosomal response to start codon recognition, the contribution of other factors in retaining eIF1 in the open complex and facilitating its release on start codon selection remains elusive. Recently, a novel role for eIF5 in antagonizing eIF1 function by promoting its release has been proposed (28), but the mechanism by which eIF5 promotes eIF1 release is unknown. Another open question is how mRNA binding to the PIC is stabilized with the mRNA entry channel open (31).

eIF4G is the major scaffolding subunit of eIF4F, linking eIF4A to the m^7G-cap of the mRNA, and thereby recruiting mRNA to the PIC (25, 44). Mammalian and most other metazoan eIF4G contain three HEAT domains, of which the first two serve as eIF4A-binding sites and the last is the binding site for Mnk eIF4E kinases (17). Yeast eIF4G lacks the last two HEAT domains, but retained the first HEAT domain, which is sufficient to bind eIF4A. Despite this structural difference, the functions of mammalian and yeast eIF4G are very similar, most notably, their ability to bind eIF4A, eIF4E and the poly(A)-binding protein (Pab). In addition, conserved RS domains of eIF4G, here termed RS1 and RS2, are located N-terminal and C-terminal to the MIF4G HEAT domain (27). While the RS1 domain of mammalian eIF4G1 is shown to promote scanning for a start

codon under the control of internal ribosome-entry site (32), the precise role of these disordered segments is unknown.

The N-terminal tail (NTT) of eIF2β contains three lysine-rich segments called K-boxes (4). eIF2β-NTT is the common binding site for eIF5 and eIF2Bε, promoting eIF2 TC recruitment to the ribosome (3) and the re-activation of eIF2 by guanine nucleotide exchange (4), respectively. Interestingly, eIF2β-NTT also binds mRNA via its K-boxes, suggesting a role for eIF2β in mRNA recruitment (20). Moreover, depletion of eIF4G in yeast does not compromise mRNA binding to the 40S subunit *in vivo*, suggesting that additional factors including eIF2 and eIF3 are involved in stably anchoring mRNA to the 40S subunit (19). Furthermore, alanine substitutions altering K-boxes increase the accuracy of start codon selection, suggesting that eIF2β is also involved in a subsequent step in AUG recognition (20). The precise roles for eIF2β K-boxes in contributing to mRNA binding to the PIC and start codon selection have not been defined.

To answer the questions mentioned above, we have studied the positively charged disordered segments of eIF4G and eIF2β, the RS1-domain of eIF4G and the K-boxes of eIF2β, which we find bind eIF1, eIF5 and mRNA (7, 14, 26). Our data indicates that eIF4G-RS1 interaction with eIF5 is directly responsible for eIF4G-mediated mRNA binding to the 43S complex, and that the eIF2β-K-boxes stabilize mRNA binding to the 40S subunit.

In selecting AUG start codons, we find that mutations of eIF4G-RS1 or eIF5 increase the accuracy of start codon. Our data supports a model whereby the eIF2β-K-boxes and eIF4G-RS1, along with, eIF5-CTD, are involved in shifting the ribosome to a

closed state after mRNA binding. Based on previous studies and the data presented here, we propose a detailed protein-protein interaction model explaining how the rearrangement of interactions involving eIF2β-NTT and eIF4G-RS1 leads to eIF1 release in response to start codon recognition.

Materials and methods

Yeast strains and methods – Plasmids used in this study, listed in Table S1, were generated as described in Supplementary text using oligodeoxyribonucelotides as listed in Table S2. The yeast *Saccharomyces cerevisiae* encodes two copies of eIF4G, eIF4G1 encoded by *TIF4631* and eIF4G2 encoded by *TIF4632*. Two series of *S. cerevisiae tif4632* strains were used in this study as listed in Table S3. One is derived from the *GCN2*$^{+}$ strain YAS1955 (column 5, Table S3) (42), which was employed to study the Gcn2p-dependent general control response to 3AT-induced histidine starvation. The other is derived from KAY220 (column 6, Table S3) (44) carrying *his4-303* with start codon altered to AUU, a phenotypic reporter for stringency of start codon selection. They were generated by introducing wild-type or mutant *HA-TIF4632 TRP1* plasmid to YAS1948 (42) and KAY173 (44), respectively, and evicting the resident *TIF4632 URA3* plasmid by the growth of the resulting transformants in the presence of FOA (plasmid shuffling).

KAY976 (*TIF5 his4-306 ura3*), KAY978 (*tif5-AN1 his4-306 ura3*), KAY979 (*tif5-AN1_ΔE396 his4-306 ura3*), KAY977 (*tif5-BN1-FL his4-306 ura3*), and KAY936 (*ssu2-1-FL his4-303 ura3*) were constructed similarly by FOA-mediated plasmid shuffling with the parental strain EY920 [*MATa ura3-52 leu2-3 leu2-112 trp1Δ-63 his4-306*(*UUG*) *tif5Δ::hisG* p(sc *URA3 TIF5*)] (37) and the single-copy *LEU2* plasmids,

YCpL-TIF5-FL (4), YCpL-tif5-AN1, YCpL-tif5-AN1_ΔE396, YCpL-tif5-BN1-FL (45) and YCpL-tif5-G62S (K. Asano, personal collection).

Standard yeast molecular biology methods including growth and β-galactosidase assays were used throughout (21).

Biochemical methods – GST pull down assays of ^{35}S-labeled proteins (36), ^{32}P-β-globin mRNA (44) and the purified 40S subunit (29) as well as ^{32}P-MFA2 mRNA recruitment assay in yeast cell extracts (5) were conducted as described.

eIF2β-dependent mRNA recruitment to the 40S subunit was assayed as follows. ^{32}P-MFA2 mRNA (24500 cpm) prepared as described (5), purified 40S subunit (0.144 A_{260} U or 240 pmol) (1) and appropriate recombinant eIF fragments (10 μg or 260 pmol of GST-eIF2β, or 8 μg or 400 pmol of His-eIF5-B6) were incubated in 50 μl binding buffer (20 mM HEPES-KOH, 75 mM KOAc, 2 mM $Mg(OAc)_2$, 1 mM EDTA, 1 mM dithiothreitol) at 4^{o}C for 90 min. Then the samples were fixed with 1% HCHO on ice for 5 min, quenched with 0.1 M glycine and layered on 5-40% sucrose gradient containing 20 mM Tris-HCl (pH7.5), 100 mM NaCl, and 1 mM $MgCl_2$. After ultracentrifugation at 39,000 rpm for 4.5 hr, the gradient sample was fractionated by ISCO gradient fractionator. A half of the fractions were used for scintillation counting and the other half used for immunoblotting with anti-SUI3 or anti-RpsO antibodies.

Results

Yeast model to study eIF4G

Like mammals, yeast encodes two copies of eIF4G, eIF4G1 and eIF4G2, highly homologous to each other. The deletion of both *TIF4631* (encoding eIF4G1) and *TIF4632* (encoding eIF4G2) is lethal (13) and either copy can complement the lethal effect of the deletion, provided that the copy is expressed from the stronger *tif4631* promoter (41). Both eIF4G1 and eIF4G2 are able to bind eIF1 and eIF5 (14, 44). Since we narrowed down the minimal eIF1- and eIF5-binding sites in eIF4G2 (14), we have chosen to study eIF4G2 in this communication and further dissect its interaction with eIF1 and eIF5. Accordingly, we used a *tif4631 tif4632* double deletion strain carrying a plasmid expressing wild-type or mutant HA-tagged eIF4G2 under the *tif4631* promoter. Fig. 1A, bottom four lines, depicts eIF4G2 alleles used in this study.

The eIF4G2 RS1 domain binds eIF1, eIF5 and mRNA

Optimal interaction of yeast eIF4G2 with eIF1 and eIF5 requires (i) its intact HEAT domain (aa. 557 –812; see Fig 1A for its location) and (ii) its Arg and Ser-rich segment (RS1) located N-terminal to the HEAT domain (14). To better characterize the RS1 segment of eIF4G2, we determined the minimal eIF1- and eIF5-binding segment of RS1 by truncation analysis and crucial amino acids therein by point mutations. Fig. 1A lists truncated versions of eIF4G2 used here for interaction assays; alphabetical designation of the fragments is used throughout the text (see Fig. 4A for additional constructs). eIF4G2_fragment B (frgB, $eIF4G2_{439\text{-}577}$) was the previously determined minimal binding segment for eIF1 and eIF5, but it still contained a part of the HEAT domain making it difficult to draw a definitive conclusion of the contribution of RS1 to eIF1 and eIF5 binding (Fig. 1B, lane 5). As shown in Fig. 1B, a GST-eIF4G2 fusion carrying only the RS1 domain (frgC, $eIF4G2_{439\text{-}513}$) was sufficient for binding to eIF1 and eIF5-CTD

(eIF5-C), which is minimally required for eIF4G2 binding. In contrast, eIF4G2-frgC did not interact with the mRNA helicase, eIF4A (Fig. 1B, autorad labeled ^{35}S-eIF4A), confirming the specificity for the interaction involving the frgC.

eIF4G2-frgC (positions 439-513) is a hydrophilic segment enriched in Arg (17%), Ser (17%), Lys (8%), Pro (8%) and Asp (9%). To determine which amino acids in RS1 are responsible for its interaction with eIF1 and eIF5, we started by examining the effect of mutations altering the most prominent category of amino acids, positively charged Arg and Lys. Thus, we created *tif4632-8** altering R473, K491 and R501 to Ile, Arg and Ser, respectively, and *tif4632-7R* altering R487, R492, R493, R496, R501, R502 and R505 all to glutamine, a similarly sized polar amino acid. The latter mutation of the RS1 domain altering the positively charged cluster, but not the former mutation, abolished its binding to eIF1 and eIF5-CTD (Fig. 1C, lanes 3-5). However, the same mutation constructed in context of the entire C-terminal portion of eIF4G2 (eIF4G2-frgA) did not abolish, but reduced the binding to these factors (Fig. 1C, lanes 6 and 7). This latter observation supports the idea that eIF4G2 has more than one region that participates in eIF1 and eIF5 binding that is dependent on the integrity of the HEAT domain (14).

Since eIF4G2-frgC also binds RNA (44), we tested the effect of *tif3632-7R* on mRNA binding by this fragment. Interestingly, *tif4632-7R* also abolished ^{32}P-labeled β-globin mRNA binding to eIF4G2-frgC, which was immobilized onto a nitrocellulose membrane (Northwestern assay; Fig. 1D, lanes 4-6). Together, these results indicate that the Arg-rich motif in the RS1 domain is responsible at least in part for its binding to eIF1, eIF5-CTD and mRNA.

eIF1 and eIF5-CTD compete for eIF4G2-RS1

Competition for binding by two distinct proteins forms the basis of remodeling protein complexes and potentially complex function via changes in protein-protein interactions. We previously showed that eIF1 and eIF5 compete for binding to the C-terminal half of eIF4G2 (eIF4G2-frgA) (14), suggesting that these factors are involved in such protein mediated remodeling. However, this experiment used a GST-eIF4G2 construct produced in a low yield, which bound only ~1% of ^{35}S-eIF5-C added (Fig. 3D in (14). Therefore, we were unable to quantitatively evaluate the competition between eIF5-C and eIF1. To overcome this problem, we tested competition with a GST-GB (streptococal protein *G B*1 domain) double fusion form of eIF4G2 that is better expressed and purifies to produce better yields of GST-eIF4G2 (44). As shown in Fig. 1E, lanes 4-5, GST-GB-eIF4G2-frgA binding to eIF5-C was strongly inhibited by His-eIF1. Similarly, GST-GB-eIF4G2-frgA binding to eIF1 was inhibited by His-eIF5-C, albeit more weakly (Fig. 1F, lanes 3-4). Importantly, eIF5-C and eIF1 also competed for binding to the minimal segment, eIF4G2-frgC (Fig. 1E, lanes 6-7; Fig. 1F, lanes 5-6), but the competition appeared to be weaker than that for eIF4G2-frgA. Together, these results confirm that the interaction of eIF4G2 with eIF1 and eIF5 are mutually competitive and also suggests that efficient competition between eIF1 and eIF5 requires the HEAT and RS2 domains.

Mutational studies indicated that the conserved acidic and basic faces of the eIF5-CTD interact with eIF4G2-frgA (45). To learn which part of eIF1 binds eIF4G2, we performed GST pull down assays with eIF1 mutant proteins bearing altered Lys-rich hydrophobic (KH), Lys- and Arg-rich (KR) surfaces of the globular domain, or NTT, of eIF1 (Fig. S1A-B). Mutations altering several amino acids in the KH and KR surfaces

abolished GST-eIF1 binding to eIF4G2-frgA (Fig. 1G, *M4* and *M5*). Conversely, GST-eIF4G2-frgA binding to eIF1 was decreased significantly by the same mutations and less profoundly by *M1*, *M2*, and *M3* altering eIF1-NTT (Fig. S1C). Thus, the KH and KR regions of eIF1 are the major eIF1 binding surfaces for eIF4G, similarly to a previous report indicating that the KH and KR regions bind to eIF5-CTD and eIF3c (34).

Three unstructured segments of yeast eIF4G2 are capable of binding RNA and involved in mRNA recruitment to the 40S subunit

To contrast the role of eIF4G2-RS1 in translation initiation with that of other RNA-binding domains of eIF4G2, we sought to identify additional RNA-binding domains in eIF4G2. We recently showed that eIF4G2-frgC encompassing RS1 and the C-terminal segment of eIF4G2 (frgH in Fig.4A) containing RS2 binds ^{32}P-β-globin mRNA in vitro (44). Of the GST-eIF4G2 fragments tested, we identified two additional fragments of eIF4G2 that influenced β-globin mRNA-binding, eIF4G2-frgG (eIF4G2$_{1-176}$), as well as a longer segment eIF4G2-frgF (eIF4G2$_{1-239}$), both of which contain a distinct RNA-binding domain located in the N-terminal region (Fig. S2A, lanes 2-3). These results localize three RNA-binding domains within eIF4G2, similar to yeast eIF4G1 (9).

To examine the *in vivo* function of individual RNA-binding domains, we generated yeast expressing eIF4G2 mutants lacking these sites as the sole copy of eIF4G. Because *tif4632-ΔA* encoding eIF4G lacking the entire C-terminal tail did not express in yeast (RW and KA, personal observations), we generated a strain bearing *tif4632-ΔX*, lacking half of RS2 to the C-terminal end of the protein (Fig. 1A). In addition, we generated strains expressing *tif4632-ΔN* lacking the N-terminal RNA-binding domain and

tif4632-7R, which alters 7 Arg amino acids that are required for binding to RNA, eIF1 and eIF5 (Fig. 1). All three alleles expressed the eIF4G2 mutants at a level equivalent to or higher than that of wild-type eIF4G2 (Fig. 2A). All strains expressing eIF4G2 mutants grew normally at a permissive temperature of 30^{o} C, but they also all grew slowly at a more restrictive temperature of 37^{o} C (see Fig. 2B, panels 1-3 for *tif4632-7R,* data not shown for others). Thus, we concluded that all RNA-binding domains of eIF4G2 play important roles in maintaining cell viability at 37°C.

Cell-free extracts were prepared from eIF4G2 mutant strains to test whether ^{32}P-labeled model mRNA (poly(A)-tailed *MFA2* mRNA) is as efficiently recruited to 40S subunits by mutant eIF4G2 proteins. Addition of non-hydrolyzable GTP analog, GMPPNP, to block hydrolysis of nucleotide bound to eIF2 allowed us to evaluate assembly of 48S complexes prior to start codon selection. All three mutants displayed a defect in stable mRNA binding to the 40S subunit (Fig. 2C and Fig. S3A for statistical analysis of binding). Minor growth defects of yeast caused by the *tif4632* mutations and reduced mRNA binding to 40S ribosomal subunits in extracts containing mutant eIF4G2 proteins suggests there is redundancy built into eIF4G2 RNA-binding for recruitment of mRNA to the 40S subunit.

Having observed the strongest mRNA-binding defect caused by *tif4632-ΔN* (Fig. S3A), we considered this may be due to alteration of the Pab1p-binding site (Fig. 1A). In agreement with this idea, recent studies on yeast eIF4G1 showed that Box 3 conserved among fungal eIF4G N-termini is responsible for Pab1p binding (30). In eIF4G2, Box 3 is located within the region deleted by *tif4632-ΔN* (labeled b3 in Fig. 1A). To test if Box 3 is required for Pab1p binding to eIF4G2, we performed a pull down assay with GST-

eIF4G2 fragments and ^{35}S-Pab1p. As shown in Fig. S2B, eIF4G2-frgF (eIF4G2$_{1-239}$) or a still longer construct, eIF4G2-frgE (eIF4G2$_{1-514}$), but not eIF4G2-frgG (eIF4G2$_{1-172}$), bound Pab1p (Fig. S2B), confirming that a region including Box 3 is the Pab1p-binding site. Thus, the N-terminal RNA- and Pab1p-binding sites are functionally conserved between yeast eIF4G1 and eIF4G2.

The eIF4G2-RS1 interaction with eIF5 mediates mRNA recruitment to the 43S complex

During the characterization of the *tif4632-7R* mutant, we found that it showed sensitivity to 3-aminotriazole (3AT), the His3p inhibitor, at the semi-restrictive temperature of 34^{o} C (Fig. 2B compare panels 2 and 4). Histidine starvation caused by 3AT activates Gcn2p eIF2α kinase, which in turn promotes translation of Gcn4p, the transcriptional activator of amino acid biosynthesis enzymes including His3p. *GCN4-lacZ* reporter assays indicated, however, that *GCN4* is normally induced by 3AT in *tif4632-7R* cells (Fig. 2D, columns 2 and 4), although the basal *GCN4* expression in the absence of 3AT was increased in these cells (columns 1 and 3; this unexpected finding is discussed below). Because *tif4632-7R* impairs mRNA-binding to the ribosome (Fig. 2C), we presumed that the 3AT-sensitivity of *tif4632-7R* would be a result of a general translation defect; a strong eIF4G function would be required to conduct general translation in the presence of 3AT, which inhibits Met-tRNA$_i^{Met}$-binding via eIF2 phosphorylation. Thus, an impaired eIF4G function would result in slower growth in the presence of 3AT. If this is the case, we reasoned that 3AT-sensitivity would be suppressed by overexpression of critical binding-partners of eIF4G2-RS1, eIF1, eIF5 and potentially eIF4A, due to mass action effects. As shown in Fig. 3A, the overexpression of eIF5, but not eIF1 or eIF4A,

suppressed the 3AT sensitivity of *tif4632-7R*. This is not simply due to a general change in growth of yeast overexpressing eIF5, since overexpression of eIF5 does not affect the growth of wild-type cells in the presence of 3AT (Fig. 3B, row 2). Thus, the eIF4G2-RS1 interaction with eIF5 mediates the critical function impaired by the *tif4632-7R* mutation.

A caveat to this interpretation was the previous observation that eIF5 overexpression can induce *GCN4* translation by inhibiting eIF2B-catalyzed eIF2 recycling by guanine nucleotide exchange, thereby converting 3AT-sensitive *gcn2Δ* strains to 3AT-resistance (Gcd^- phenotype, Fig. 3B, panel 4, rows 7-8) (38). Thus, eIF5 overexpression in *tif4632-7R* cells could potentially increase 3AT-resistance by constitutively expressing *GCN4* without restoring defective eIF4G2 function. To rule out this possibility, we examined the effect of *tif5-Δ20*, a deletion of a 20 amino acid-long segment of eIF5 that was recently identified as a segment inhibiting GDP release from eIF2 (GDI activity) (18). The GDI activity of eIF5 antagonizes eIF2B-mediated eIF2 re-activation; thus deletion of this domain eliminates the effect of eIF5 to decrease ternary complex (TC) abundance, and hence its ability to confer 3AT-resistance (Fig. 3B, panel 4, rows 8-9) without changing the eIF5 expression level (Fig. 3B panel 5). The overexpression of eIF5-Δ20 still suppressed the 3AT-sensitivity by *tif4632-7R* (Fig. 3B, rows 5-6), in support of the idea that the phenotype was suppressed by eIF5 mass action, but not by enhancing *GCN4* induction through TC levels.

To directly test if the eIF4G2-RS1 interaction with eIF5 mediates mRNA recruitment to the ribosome, we examined the effect of eIF5 addition on the ^{32}P-*MFA2* mRNA recruitment defect observed in eIF4G2-7R cell extracts. The addition of eIF5 restored the mRNA binding defect that was observed in the mutant extracts (Fig. 3C, see

Fig. S3B for statistical analysis), demonstrating that the eIF4G2-RS1 interaction with eIF5 mediates mRNA recruitment to the ribosome. The restoration of mRNA recruitment under these conditions is specific to eIF5, because addition of eIF1 did not restore mRNA binding (Fig. S4A), and addition of eIF5-C did not restore the mRNA binding defect (Fig. S4B), indicating that the eIF5-CTD is not sufficient to mediate stable complex formation with mRNA.

eIF5 stimulates mRNA binding by eIF4G in vitro

In an effort to delineate the mechanism by which eIF4G interaction with eIF5 promotes mRNA binding by the 43S complex, it was found that the addition of full-length eIF5 or eIF5-C (CTD) increases ^{32}P-β-globin mRNA binding to eIF4G2-frgA by 2-fold (Fig. 4A, rows 1 and 2). GST-pull down assays were used with recombinant GST-eIF4G2 and ^{32}P-β-globin mRNA to tease apart the contribution provided by eIF5 and eIF4G2 on mRNA binding to the ribosome. Each of the recombinant GST-eIF4G2 constructs used here bound 10-20% of the ^{32}P-mRNA in the absence of eIF5 (Fig. S5A). To ensure accurate comparison, the glutathione resin bound to GST fusion proteins was divided equally into two tubes, eIF5 proteins (10 μg) added to one tube and then the pull down assay was performed for both the tubes (Fig. S5B). We column-purified the longer GST-eIF4G2 species to eliminate perturbation from contaminating shorter species (Fig. S5C). Because eIF5-C can bind eIF4G2-frgC (RS1 alone) (Fig. 1) but does not stimulate its binding to ^{32}P-mRNA (Fig. 4A, row 3), the increased mRNA binding by eIF4G2-frgA is not due to eIF5 interaction with the RS1 domain *per se*, but presumably involves the HEAT and RS2 domains. ^{32}P-mRNA-binding to eIF4G2-frgH (RS2 alone) or eIF4G2-frgD (HEAT

plus RS2) was not affected by eIF5-C (Fig. 4A, rows 4-5), consistent with their inability to bind eIF5 (14). Interestingly, partial or complete elimination of RS2 in eIF4G2-frgI or to eIF4G2-frgJ, respectively, not only abolished the ability of eIF5 to stimulate mRNA binding to eIF4G2, but it also rendered eIF5 inhibitory to mRNA binding by eIF4G2 (Fig. 4A, rows 6-7). Since eIF5 did not inhibit mRNA binding by eIF4G2-frgC, the eIF5 inhibition of mRNA binding by eIF4G-frgI and –frgJ appears to involve the HEAT domain. These results indicate that the RS2 domain is required for the eIF5-stimulated mRNA binding by eIF4G2 and also suggest that this process involves eIF5 interaction with the HEAT domain.

eIF5 antagonizes eIF2β-dependent mRNA binding to the 40S subunit

In addition to the eIF4G2 RS domains, the eIF2β K-box segment alone can bind mRNA, and its role in mRNA recruitment to the ribosome was postulated (20). In contrast to its effect on mRNA binding by eIF4G2, eIF5-C reduced the efficiency of eIF2β binding to ^{32}P-mRNA by 2 fold (Fig. 4A, row 7). To address whether this observation relates to the ability of eIF2β to mediate mRNA binding to the ribosome, we first tested if eIF2β-NTT can bind directly to the 40S subunit. As shown in Fig. 3B, lane 3, middle gel, GST-eIF2β-N (eIF2$\beta_{1\text{-}140}$) carrying all the three K-boxes bound the 40S subunit purified from wild-type yeast. As a control, GST-eIF1 bound the 40S subunit (lane 5) as shown previously (29). This K-box-40S subunit interaction was not impeded by an excess amount of non-radiolabeled β-globin mRNA (Fig. 4B), ruling out that the interaction is due to general RNA-binding activity of the K-boxes. More importantly, this interaction was significantly decreased by the 18S rRNA *A1193U* mutation (29) altering the 40S

subunit P-site (Fig. 4B and 4C). Thus, the eIF2β K-box segment alone interacts with the 40S subunit, and this interaction specifically depends on the intact structure of the 40S subunit decoding site.

Having observed that the eIF2β segment containing K-boxes bind mRNA and the 40S subunit and that the mRNA in excess did not inhibit eIF2β binding to the 40S subunit, it was conceivable that the eIF2β segment alone can serve as a bridge between mRNA and the 40S subunit. To test this idea, we incubated the 40S subunit and ^{32}P-*MFA2* mRNA in the absence or presence of GST-eIF2β-N and examined if the eIF2β protein increases mRNA bound to the ribosome in a sucrose gradient-velocity sedimentation analysis (see Materials and methods). Immunoblot analysis of the gradient fractions indicated that GST-eIF2β-N comigrates with the 40S subunit confirming the mutual interaction between eIF2β-N and the 40S subunit (Fig. 5A, panel 2, bottom gel). Scintillation counting of the gradient fractions showed that GST-eIF2β-N increases ^{32}P-*MFA2* mRNA binding to the 40S subunit (Fig. 5B and 5C). Importantly, the addition of eIF5-C to the preformed complexes significantly decreased eIF2β-stimulated ^{32}P-mRNA recruitment (Fig. 5B and 5C) without affecting the amount of GST-eIF2β-N comigrating with the 40S subunit (Fig. 5A, panel 3). Thus, eIF5-C specifically inhibits mRNA binding by eIF2β, but not 40S subunit binding by eIF2β (Fig. 5D). These results suggest that the eIF2β-K-box segment can promote mRNA recruitment to the 40S subunit and that this recruitment is favored in the absence of eIF5-CTD:eIF2β-K-boxes interaction (see Discussion).

eIF4G2-RS1 is involved in the 48S PIC commitment to initiation in response to start codon selection

Our *GCN4-lacZ* reporter assay showed that *tif4632-7R* significantly increased *GCN4* expression in the absence of starvation signals (Fig. 2D). Translation of *GCN4* mRNA is normally blocked by re-initiation of translation at uORF elements in the 5`-leader region, which leads to ribosome dissociation (15). The starvation-induced eIF2 phosphorylation inhibits eIF2 re-activation and decreases eIF2/GTP/Met-tRNA$_i^{Met}$ TC abundance, thereby allowing the 40S ribosome to bypass the inhibitory uORFs and re-initiate at *GCN4* AUG. Mutations impairing TC loading or retention on the 40S subunit mimic the effect of eIF2 phosphorylation, thereby increasing *GCN4* expression in the absence of inducing signals (general control derepressed or Gcd$^-$ phenotype) (6). Therefore, our finding indicates that eIF4G2-*7R* confers a Gcd$^-$ phenotype, suggesting that this mutation destabilizes TC binding to the 40S subunit.

To get more insights into the role of eIF4G2-RS1 during the PIC function in vivo, we examined translation from UUG a non-canonical start codon. If an eIF mutation relaxes the stringency of start codon selection, it allows translation initiation of a reporter gene where the start codon has been switched from AUG to UUG, the *su*ppressor of *i*nitiation codon mutation phenotype (Sui$^-$). If the mutation increases the accuracy of translation initiation, it suppresses the relaxed stringency of initiation caused by a Sui$^-$ mutation (Suppressor of Sui or Ssu$^-$ phenotype) (6, 12, 35). Recent studies indicate that mutations impairing the open state of the PIC tend to relax stringent AUG selection by allowing the PIC to achieve the closed state at a UUG codon (Sui$^-$ phenotype), while mutations impairing closed state tend to increase the stringency of initiation by inhibiting

formation of the PIC to the closed state at a UUG codon (Ssu$^-$ phenotype) (35). Since *tif4632-7R* conferred a Gcd$^-$ phenotype suggesting destabilization of the scanning ribosomal complex, it was anticipated that this mutation also displays Sui$^-$ or Ssu$^-$ phenotype. To test whether *tif4632-7R* would confer Sui$^-$ or Ssu$^-$ phenotype, we introduced this allele into yeast carrying a *his4-303* allele, in which the start codon was altered to AUU. As shown in Fig. 6A, row 3, *tif4632-7R* did not promote His4p expression, and hence was judged to be Sui$^+$ (16). In contrast, we found that *tif4632-7R* suppressed the Sui$^-$ phenotype caused by *SUI3-2* (Fig. 6A, row 3; Ssu$^-$ phenotype).

To confirm that the Ssu$^-$ phenotype is due to altered translation from *his4-303*, we transformed the *tif4632-7R* mutant with plasmids carrying *HIS4-lacZ* reporters, either with its natural start codon (*HIS4^{AUG}-lacZ*), or with a AUU start codon in *his4-303* (*HIS4^{AUU}-lacZ*). *tif4632-7R* significantly increased expression from *HIS4^{AUG}-lacZ* compared to wild-type ($p = 0.015$; Fig. 6B, columns 6 and 8). This is consistent with increased *GCN4* expression or Gcd$^-$ phenotype of this mutant without inducing amino acid starvation (Fig. 2D); because Gcn4p is an activator of *HIS4* transcription, the reporter expression was likely due to increased transcription. Similar observations were made with Gcd$^-$ mutations altering eIF2γ (11). With *tif4632-7R* decreasing the relative frequency of translation initiation from the UUG codon (UUG/AUG ratio in Fig. 6C, columns 3-4), we conclude that eIF4G2-RS1 is important for 48S PIC commitment to initiation at the non-cognate start codon.

eIF2β-, eIF4G- and eIF3c-binding faces of eIF5-CTD are also involved in the 48S PIC commitment to initiation at a UUG codon

The Ssu$^-$ phenotype observed with *tif4632-7R* is akin to the phenotype caused by a K-box mutation that alters eIF2β-NTD (20). The common protein partners of these protein segments are eIF1 and eIF5. Many mutations altering eIF1 cause increased tolerance of non-cognate start-codon usage, suggesting that interactions of eIF1 and other translation initiation factors contribute to stabilizing the open state of a PIC-phase ribosome (6). We wished to examine more closely how abolishing eIF5-CTD interactions with its known binding partners affects the formation of the closed state of the PIC. *tif5-AN1* alters the acidic Area I of eIF5-CTD and *ΔE396* eliminates E396 and the acidic C-terminal tail. The former mutation reduces the eIF5 interaction with eIF2β, while the double mutation *AN1_ΔE396* does so to a larger extent (45). *tif5-AN1* also reduces the interaction with eIF4G2 (45). *tif5-BN1* changes the basic Area II of eIF5-CTD, disrupting the interaction with eIF3c and eIF1 (45). As a control, *tif5-G62S* that decreases the eIF5 GAP activity (7) displayed a Ssu$^-$ phenotype in our assay (Fig. 6D, panels 2-3, rows 1 and 9). As shown in Fig. 6D, panels 2-3, rows 5, 3, and 7, *AN1* weakly, the double mutant *AN1_ΔE396* and *BN1* still more strongly suppressed the His$^+$ phenotype caused by the eIF2β mutation *SUI3-2* (Ssu$^-$ phenotype). Thus, similar to eIF2β-K-box (20) and eIF4G2-RS1 (Fig. 6A-C) mutations, mutations at the acidic faces of eIF5-CTD interacting with these proteins displayed Ssu$^-$ phenotype. Unexpectedly, we also found that the basic face of eIF5-CTD involved in eIF3c and eIF1 binding also displayed Ssu$^-$ phenotype (see Discussion). These results support the model that the mutual interactions of eIF5-CTD with eIF2β-K-boxes and eIF4G2-RS1 are involved in the 48S PIC commitment to initiation , presumably driving the PIC to the closed state.

Discussion

In this communication, we report that yeast eIF4G2 contains three distinct RNA-binding sites (Fig. 1A), and that the RS1 domain plays a unique role in mRNA recruitment to the ribosome. The eIF4G2-RS1-mediated mRNA recruitment involves interaction with eIF5 (Fig. 1 and 3). *tif4632-7R* altering eIF4G2-RS1 reduced ^{32}P-mRNA binding to the 40S subunit in cell extracts, which was reversed by adding excess eIF5 (Fig. 3C), demonstrating that a weakened interaction with eIF5 is responsible for the mRNA binding defect. eIF5 is a component of 43S PIC (3), and here we show it increases mRNA binding to eIF4G2 containing RS1, HEAT and RS2 domains (Fig. 4A). Our data demonstrates that eIF5 stabilize the 48S PIC by enhancing eIF4G interaction with the mRNA, in addition to serving as a bridge to eIF4F:mRNA complexes.. The eIF5-stimulated RNA binding by eIF4G2 requires the RS2 domain, which is located C-terminal to the RS1 and HEAT domains. Thus, eIF5 binding through the RS1 and HEAT domains regulates RNA binding activity of RS2 that is located "at a distance" from RS1 in terms of the primary structure.

Of note was the finding that *tif4632-7R* reverses the relaxed stringency of AUG selection caused by eIF2β-S254Y (Ssu$^-$ phenotype). Ssu$^-$ phenotypes are thought to be caused by mutations impairing transition of PIC to the closed state(12). eIF1 is proposed to be a key element in repressing transition of the PIC from the open to closed state (10). Because the eIF4G-binding face of eIF1 (Fig. 1G and S2) overlaps its ribosome-binding face (KR area includingK60) (33), a mechanism to explain the Ssu$^-$ phenotype of eIF4G-RS1 mutation is that, in response to AUG recognition, eIF4G-RS1 (together with the HEAT domain) excludes eIF1 from the P-site by competitively inhibiting its binding to the ribosome. Because eIF1 appears to inhibit eIF4G2-frgA (RS1-HEAT-RS2) binding to

eIF5-CTD more strongly than it did for eIF4G2-frgC (RS1 only) (Fig. 1E), the ability to exclude eIF1 would be stronger with the intact eIF4G containing the HEAT domain. Prior to AUG recognition, eIF4G-RS1 is likely to be bound to eIF5-CTD, enhancing a stable anchoring of mRNA to the 40S subunit decoding site. Thus, it is reasonable to propose that switching eIF4G interaction with eIF5-CTD to eIF1 is an important step in promoting eIF1 release.

In strong support for a model where factor remodeling facilitates eIF1 release, in collaboration we recently showed that a eIF5-CTD mutation disrupting binding to eIF2β impaired PIC transition to the closed state *in vitro*, and it also displayed a Ssu$^-$ phenotype in combination with eIF2β-S264Y, eIF1-93-97, or eIF1-K60E *in vivo* (23). It was postulated that eIF2β-NTT is not bound to eIF5-CTD in the open state, in agreement with a model that eIF2β can stabilize mRNA binding at this stage (Fig. 5). Start-codon recognition is proposed to promote eIF2β-NTT binding of eIF5-CTD, which disrupts a network of factor interactions that anchor eIF1 to the 40S subunit, and thereby drives PIC to the closed state by facilitating eIF1 release. The Ssu$^-$ phenotypes caused by mutations altering eIF2β-K-boxes (20) and eIF5-CTD Area I and acidic tail (eIF2β-binding site) (Fig. 6D, rows 3-5) support this model. The *in vitro* reconstitution system used in this study does not include eIF4G and eIF3. However, Ssu$^-$ phenotypes caused by eIF4G-RS1 (this study) or eIF3c-NTT (43) (see below) suggest strongly that factor remodeling involving disordered segments of these factors can facilitate eIF1 release, as proposed above for eIF4G-RS1.

Similar to eIF4G-RS1, the NTT of the c subunit of eIF3 (eIF3c/Nip1p) also interacts with the KR area of eIF1. The eIF3c-NTT contains three distinct ten-aa.-long elements, Box-2, Box-6 and Box-12 (43). Of these Box-6 and Box-12 are likely to be eIF1-binding sites, since substitution of these ten-aa strongly reduced eIF1 binding by each one (12-fold and 5-fold, respectively) (43). The interaction of eIF1 with these motifs presumably helps to dissociate eIF1 from the ribosomal P-site by competitive inhibition. In support of this model, a mutation altering Box-6 restores the stringency caused by a Sui$^-$ mutation to favor AUG selection (Ssu$^-$) (43). Box-12 mutation shows a Sui$^-$ phenotype, suggesting that eIF1-binding to this element helps anchor eIF1 within the open PIC. Finally, mutational studies also suggest that Box-2 and Box-6 are eIF5-binding sites (43). Together with the Ssu$^-$ phenotype caused by *tif5-BN1* (Fig. 6D) disrupting eIF5 binding to eIF1 and eIF3c (45), these findings suggest that eIF5:eIF3c interaction is required for the shift to PIC closed state.

In conclusion, we propose that the myriad of eIF interactions, as depicted in Fig. 7a, can be sorted into two distinct sets of interactions, which characterize the open and closed states of the PIC. In the closed PIC, the key interaction is eIF1-KR binding to eIF3c-NTT and eIF4G-RS1, which together help to exclude eIF1 from the ribosome (dotted light blue lines in the bottom of Fig. 7c). Because eIF1 can bind simultaneously to eIF3c and eIF4G (14), eIF1 may dissociate from the ribosome in complex with eIF3 and eIF4G. Alternatively, eIF4G-RS1 may help eIF1 to dissociate from eIF3 after eIF1 release. The interaction between eIFs found in the open PIC is proposed to prevent these interactions, while helping eIF1 anchored to the PIC (dotted purple lines in Fig. 7b). The data presented in this report indicate that the positively charged segments, eIF4G-RS1, -

RS2 (not shown in Fig. 7b) and eIF2β-NTT (K-boxes) stabilize mRNA binding to the ribosome (orange arrows in Fig. 7b). We propose that eIF5-CTD is bound to eIF3c-NTT at this stage, positioning the latter in proximity to eIF1. In this way, eIF5-CTD:eIF3c-NTT interaction would promote eIF1 release (dotted light blue lines in Fig. 7b), which would be initiated through eIF2β-NTT binding to the eIF5-CTD (Fig. 7c). The evidence for the involvement of eIF4G-RS1 interaction with eIF3c-NTT is indirect; validating this model will require further work.

Acknowledgment

We thank Alan Hinnebusch for anti-SUI3 antibodies and stimulating discussions, Leos Valasek for anti-RpsO antibodies, Tom Donahue for anti-eIF5 antibodies, Stefan Rothenberg, Chris Fraser and John Hershey for comments on the manuscript, Gerhard Wagner, Alan Hinnebusch and Jon Lorsch for discussion and sharing results prior to publication. This work was supported by NIH GM64781 and K-state Terry Johnson Cancer Center to KA.

References

1. **Acker, M. G., S. E. Kolitz, S. F. Mitchell, J. S. Nanda, and J. R. Lorsch.** 2007. Reconstitution of yeast translation initiation. Methods Enzymol **430:**111-145.
2. **Algire, M. A., D. Maag, and J. R. Lorsch.** 2005. Pi release from eIF2, not GTP hydrolysis, is the step controlled by start-site selection during eukaryotic translation initiation. Mol Cell **20:**251-262.
3. **Asano, K., J. Clayton, A. Shalev, and A. G. Hinnebusch.** 2000. A multifactor complex of eukaryotic initiation factors eIF1, eIF2, eIF3, eIF5, and initiator $tRNA^{Met}$ is an important translation initiation intermediate in vivo. Genes Dev **14:**2534-2546.
4. **Asano, K., T. Krishnamoorthy, L. Phan, G. D. Pavitt, and A. G. Hinnebusch.** 1999. Conserved bipartite motifs in yeast eIF5 and eIF2Bε, GTPase-activating

and GDP-GTP exchange factors in translation initiation, mediate binding to their common substrate eIF2. EMBO J **18:**1673-1688.

5. **Asano, K., P. Lon, T. Krishnamoorthy, G. D. Pavitt, G. E., E. M. Hannig, J. Nika, T. F. Donahue, H.-K. Huang, and A. G. Hinnebusch.** 2002. Analysis and Reconstitution of Translation Initiation In Vitro. Methods in Enzymology **351:**221-247.
6. **Asano, K., and M. S. Sachs.** 2007. Translation factor control of ribosome conformation during start codon selection. Genes Dev **21:**1280-1287.
7. **Asano, K., A. Shalev, L. Phan, K. Nielsen, J. Clayton, L. Valasek, T. F. Donahue, and A. G. Hinnebusch.** 2001. Multiple roles for the carboxyl terminal domain of eIF5 in translation initiation complex assembly and GTPase activation. EMBO Journal **20:**2326-2337.
8. **Asano, K., H.-P. Vornlocher, N. J. Richter-Cook, W. C. Merrick, A. G. Hinnebusch, and J. W. B. Hershey.** 1997. Structure of cDNAs encoding human eukaryotic initiation factor 3 subunits: possible roles in RNA binding and macromolecular assembly. J Biol Chem **272:**27042-27052.
9. **Berset, C., A. Zurbriggen, S. Djafarzadeh, M. Altmann, and H. Trachsel.** 2003. RNA-binding activity of translation initiation factor eIF4G1 from Saccharomyces cerevisiae. RNA **9:**871-880.
10. **Cheung, Y.-N., D. Maag, S. F. Mitchell, C. A. Fekete, M. A. Algire, J. E. Takacs, N. Shirokikh, T. Pestova, J. R. Lorsch, and A. Hinnebusch.** 2007. Dissociation of eIF1 from the 40S ribosomal subunit is a key step in start codon selection in vivo. Genes Dev **21:**1217-1230.
11. **Dorris, D. R., F. L. Erickson, and E. M. Hannig.** 1995. Mutations in *GCD11*, the structural gene for eIF-2γ in yeast, alter translational regulation of *GCN4* and the selection of the start site for protein synthesis. EMBO J **14:**2239-2249.
12. **Fekete, C. A., S. F. Mitchell, V. A. Cherkasova, D. Applefield, M. A. Algire, D. Maag, S. A. K, J. R. Lorsch, and A. Hinnebusch.** 2007. N-and C-terminal residues of eIF1A have opposing effects on the fidelity of start codon selection. EMBO J **26:**1602-1614.
13. **Goyer, C., M. Altmann, H. Trachsel, and N. Sonenberg.** 1989. Identification and characterization of cap binding proteins from yeast. J Biol Chem **264:**7603-7610.
14. **He, H., T. von der Haar, R. C. Singh, M. Ii, B. Li, A. G. Hinnebusch, J. E. G. McCarthy, and K. Asano.** 2003. The yeast eIF4G HEAT domain interacts with eIF1 and eIF5 and is involved in stringent AUG selection. Molecular and Cellular Biology **23:**5431-5445.
15. **Hinnebusch, A. G., T. E. Dever, and K. Asano.** 2007. Mechanism of translation initiation in the yeast Saccharomyces cerevisiae, p. 225-268. *In* M. B. Mathews, N. Sonenberg, and J. W. B. Hershey (ed.), Translational Control in Biology and Medicine. Cold Spring Harbor Lab Press, Cold Spring Harbor, NY.
16. **Huang, H., H. Yoon, E. M. Hannig, and T. F. Donahue.** 1997. GTP hydrolysis controls stringent selection of the AUG start codon during translation initiation in *Saccharomyces cerevisiae*. Genes Dev **11:**2396-2413.

17. **Jackson, R. J., C. U. T. Hellen, and T. V. Pestova.** 2010. The mechanism of eukaryotic translation initiation and principles of its regulation. Nat Rev Mol Cell Biol **10:**113-127.
18. **Jennings, M. D., and G. D. Pavitt.** 2010. eIF5 has GDI activity necessary for translational control by eIF2 phosphorylation. Nature **465:**378-381.
19. **Jivotovskaya, A. L., L. Valasek, A. G. Hinnebusch, and K. H. Nielsen.** 2006. eIF3 and eIF2 can promote mRNA binding to 40S subunits independently of eIF4G in yeast. Mol Cell Biol **26:**1355-1372.
20. **Laurino, J. P., G. M. Thompson, E. Pacheco, and B. A. Castilho.** 1999. The β subunit of eukaryotic translation initiation factor 2 binds mRNA through the lysine repeats and a region comprising the C_2-C_2 motif. Molecular and Cellular Biology **19:**173-181.
21. **Lee, B., T. Udagawa, C. S. Singh, and K. Asano.** 2007. Yeast phenotypic assays on translational control. Methods Enzymol **429:**139-161.
22. **Lorsch, J. R., and T. E. Dever.** 2010. Molecular view of 43S complex formation and start site selecion in eukaryotic translation initiation. J Biol Chem **285:**21203-21207.
23. **Luna, R. E., H. Arthanari, H. Hiraishi, J. Nanda, P. Martin-Marcos, M. Markus, B. Arabayov, A. Milbradt, S. Hyperts, L. E. Luna, M. Reibarkh, D. Miles, A. Farmy, H.-C. Seo, A. Marintchev, A. G. Hinnebusch, J. R. Lorsch, K. Asano, and G. Wagner.** 2012. The C-terminal domain of eukaryotic initiation factor 5 promotes start codon recognition by its dynamic interplay with eIF1 and eIF2 β Cell Reports **in press**.
24. **Luna, R. E., H. Arthanari, H. Hiraishi, J. Nanda, P. Martin-Marcos, M. Markus, B. Arabayov, A. Milbradt, S. Hyperts, L. E. Luna, M. Reibarkh, D. Miles, A. Farmy, H.-C. Seo, A. Marintchev, A. G. Hinnebusch, J. R. Lorsch, K. Asano, and G. Wagner.** Submitted. The C-terminal domain of eukaryotic initiation factor 5 promotes start codon recognition by its dynamic interplay with eIF1 and eIF2 β
25. **Marintchev, A., K. A. Edmonds, B. Maritcheva, E. Hendrickson, M. Oberer, C. Suzuki, B. Herby, N. Sonenberg, and G. Wagner.** 2009. Topology and regulation of the human eIF4A/4G/4H helicase complex in translation initiation. Cell **136:**447-460.
26. **Mitchell, S. F., W. S. E, M. A. Algire, E. H. Park, A. G. Hinnebusch, and J. R. Lorsch.** 2010. The 5`-7-methylguanosine cap on eukaryotic mRNAs serves both to stimulate canonical translation initiation and to block an alternative pathway. Mol Cell **39:**950-962.
27. **Morley, S. J., P. S. Curtis, and V. M. Pain.** 1997. eIF4G: translation's mystery factor begins to yield its secrets. RNA **3:**1085-1104.
28. **Nanda, J. S., Y.-N. Cheung, J. E. Takacs, P. Martin-Marcos, A. K. Saini, A. G. Hinnebusch, and J. R. Lorsch.** 2009. eIF1 controls multiple steps in start codon recognition during eukaryotic translation initiation. J Mol Biol **394:**268-285.
29. **Nemoto, N., T. Udagawa, C. R. Singh, S. Wang, E. Thorson, Z. A. Winter, T. Ohira, S. J. Brown, and K. Asano.** 2010. Yeast 18S rRNA is directly involved

in the ribosomal response to stringent AUG selection during translation initiation. J Biol Chem **285:**32200-32212.

30. **Park, E. H., S. E. Walker, J. M. Lee, S. Rothenburg, J. R. Lorsch, and A. G. Hinnebusch.** 2011. Multiple elements in the eIF4G1 N-terminus promote assembly of eIF4G1•PABP mRNPs in vivo. EMBO J **30:**302-316.
31. **Passmore, L. A., T. M. Schmeing, D. Maag, D. J. Applefield, M. G. Acker, M. A. Algire, J. R. Lorsch, and V. Ramakrishnan.** 2007. The eukaryotic translation initiation factors eIF1 and eIF1A induce an open conformation of the 40S ribosome. Mol Cell **26:**41-50.
32. **Prevot, D., D. Decimo, C. H. Herbreteau, F. Roux, J. Garin, J.-L. Darlix, and T. Ohlmann.** 2003. Characterization of a novel RNA-binding region of eIF4GI critical for ribosomal scanning. EMBO J **22:**1909-1921.
33. **Rabl, J., M. Leibundgut, S. F. Ataide, A. Haag, and N. Ban.** 2011. Crystal structure of the eukaryotic 40S ribosomal subunit in complex with initiaiton factor 1. Science **331:**730-736.
34. **Reibarkh, M., Y. Yamamoto, C. R. Singh, F. d. Rio, A. Fahmy, B. Lee, R. E. Luna, M. Ii, G. Wagner, and K. Asano.** 2008. Eukaryotic initiation factor (eIF) 1 carries two distinct eIF5-binding faces important for multifactor assembly and AUG selection J Biol Chem **283:**1094-1103.
35. **Saini, A. K., J. S. Nanda, J. R. Lorsch, and A. G. Hinnebusch.** 2010. Regulatory elements in eIF1A control the fidelity of start codon selection by modulating tRNAiMet binding to the ribosome. Genes Dev **24:**97-110.
36. **Singh, C. R., and K. Asano.** 2007. Localization and characterization of protein-protein interaction sites. Methods Enzymol **429:**139-161.
37. **Singh, C. R., C. Curtis, Y. Yamamoto, N. S. Hall, D. S. Kruse, E. M. Hannig, and K. Asano.** 2005. eIF5 is critical for the integrity of the scanning preinitiation complex and accurate control of GCN4 translation. Molecular and Cellular Biology **25:**5480-5491.
38. **Singh, C. R., B. Lee, T. Udagawa, S. S. Mohammad-Qureshi, Y. Yamamoto, G. D. Pavitt, and K. Asano.** 2006. An eIF5/eIF2 complex antagonizes guanine nucleotide exchange by eIF2B during translation initiation. EMBO J **25:**4537-4546.
39. **Siridechadilok, B., C. S. Fraser, R. J. Hall, J. A. Doudna, and E. Nogales.** 2005. Structural roles for human translation factor eIF3 in initiation of protein synthesis. Science **310:**1513-1515.
40. **Sokabe, M., C. S. Fraser, and J. W. Hershey.** 2012. The Human Translation Initiation Multi-Factor Complex Promotes Methionyl-tRNAi Binding to the 40S Ribosomal Subunit. Nucl Acids Res **40:**905-913.
41. **Tarun, S. Z., and A. B. Sachs.** 1996. Association of the yeast poly(A) tail binding protein with translation initiation factor eIF-4G. EMBO J **15:**7168-7177.
42. **Tarun, S. Z., and A. B. Sachs.** 1997. Binding of eukaryotic translation initiation factor 4E (eIF4E) to eIF4G represses translation of uncapped mRNA. Molecular and Cellular Biology **17:**6876-6886.
43. **Valásek, L., K. H. Nielsen, F. Zhang, C. A. Fekete, and A. G. Hinnebusch.** 2004. Interaction of eIF3 subunit NIP1/c with eIF1 and eIF5 promote

preinitiation complex assembly and regulate start codon selection. Molecular and Cellular Biology **24:**9437-9455.

44. **Watanabe, R., M. J. Murai, C. R. Singh, S. Fox, M. Ii, and K. Asano.** 2010. The eIF4G HEAT domain promotes translation re-initiation in yeast both dependent on and independent of eIF4A mRNA helicase. J Biol Chem **285:**21922-21933.

45. **Yamamoto, Y., C. R. Singh, A. Marintchev, N. S. Hall, E. M. Hannig, G. Wagner, and K. Asano.** 2005. The eukaryotic initiation factor (eIF) 5 HEAT domain mediates multifactor assembly and scanning with distinct interfaces to eIF1, eIF2, eIF3 and eIF4G. Proc Natl Acad Sci USA **102:**16164-16169.

Figures

Figure 1

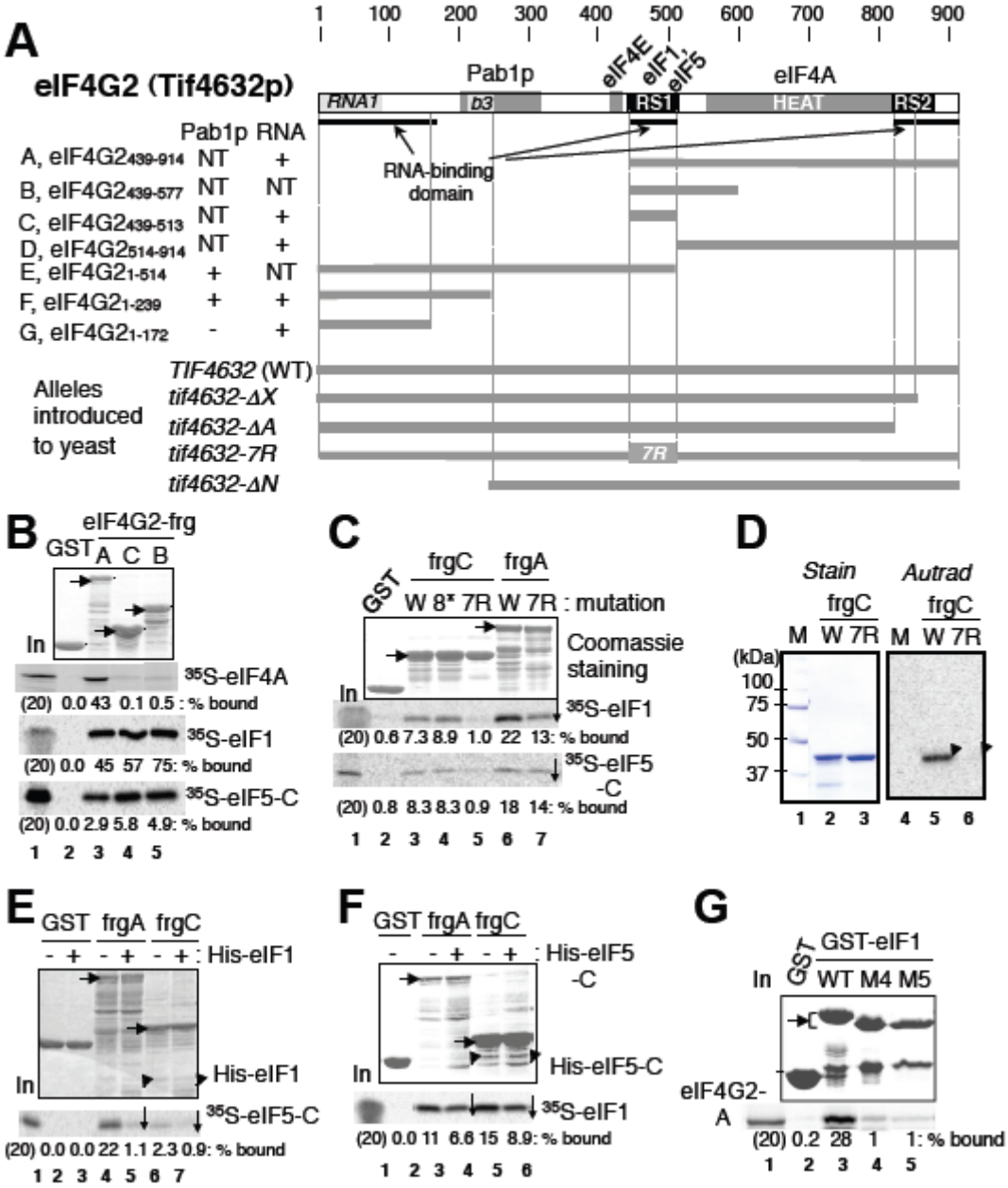

Fig. 1. Minimal binding domains of eIF4G2 (Tif4632p) for eIF1, eIF4A, eIF5 and mRNA. (A) Primary structure of yeast eIF4G2 mutations used in this study with defined binding sites for Pab1p, eIF4A, eIF4E (*gray boxes*) and bold underlines denoting RNA

binding segments. Dark boxes indicate the RS domains for RNA binding (44). Light gray boxes are homologous to *RNA1,* an RNA-binding domain in yeast eIF4G1 (9) and Box 3 displaying high homology among fungal eIF4G (*b3*) (30). Tables to the left summarizes the results of interaction assays with RNA and Pab1p; NT, not tested. (B, C, E and F) GST-eIF4G2 fusion proteins (2-5 μg of full-length products indicated by arrowheads in top gel) across the top were bound to ^{35}S-labeled proteins synthesized in rabbit reticulocyte lysate in 200-μl binding buffer. GST fusion-containing complexes together with 20% input amounts of the reaction mixtures were analyzed by SDS-PAGE followed by Coomassie staining (top panels) and autoradiography (bottom panels). Horizontal arrows indicate the full-length products. Downward arrow indicates reproduced decrease in the interaction compared to control (n=3). (B) Binary interactions of GST or indicated GST-eIF4G2 segments with ^{35}S-eIF4A, eIF1 and eIF5-C. (C) The effect of RS1 mutations *tif4632-8** (8*) or *-7R* (7R) as defined in Table S3 on eIF4G2 binding to eIF1 and eIF5. W, wild-type. (D) The effect of *tif4632-7R* on GST-eIF4G-C binding to ^{32}P-β-globin mRNA, as examined by Northwestern blot experiment (8). Left, Coomassie staining of proteins used. Right, autoradiography of proteins bound to ^{32}P-β-globin mRNA. Arrowheads, locations of full-length products. W, wild-type. (E, F) Indicated GST-eIF4G2 proteins were bound to ^{35}S-eIF5-C in the presence of 20 μg His-eIF1 (E) or ^{35}S-eIF1 in the presence of 20 μg His-eIF5-C (F). Arrowheads, locations of His-eIF1 or His-eIF5-C bound. (G) GST-eIF1 and its M4 and M5 mutant derivatives were allowed to bind ^{35}S-eIF4G2-A and the ^{35}S-proteins bound were analyzed together with 20% in-put amount (lane 1).

Figure 2

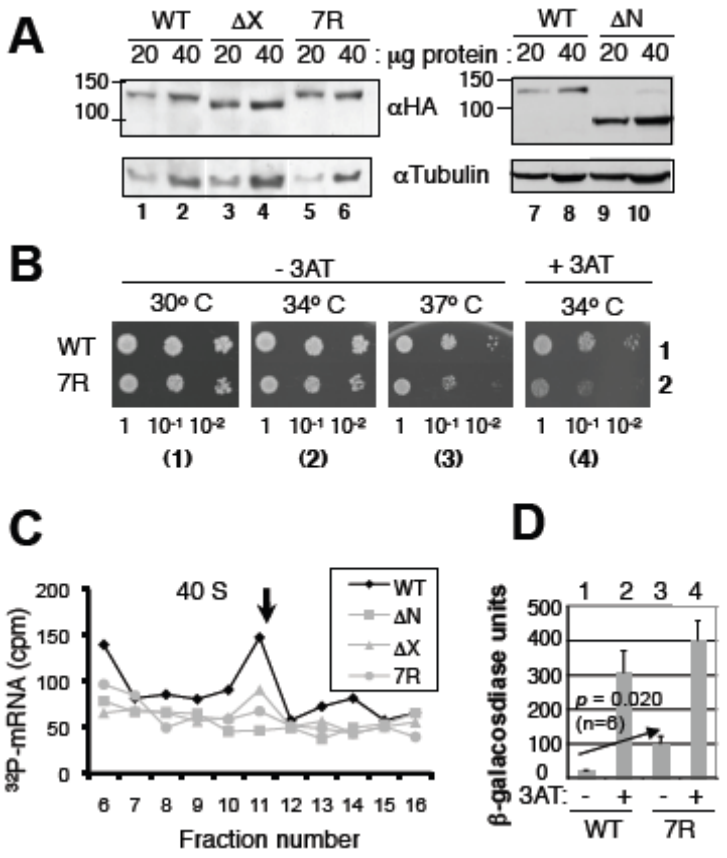

Fig. 2. Yeast phenotypes of mutants with altered RNA-binding sites of eIF4G2. (A) The expression of eIF4G2 mutants used in this study (YAS1955 derivatives; see Table S3 and Fig. 1A). 20 and 40 µg total protein from whole cell extracts of indicated strains were used for immunoblotting with anti-HA (to detect HA-eIF4G2) and anti-Tubulin antibodies (loading control). (B) Temperature- and 3AT-sensitive growth of *tif4632-7R* was assayed by spotting 5 µl 0.15 A_{600} unit culture (1) and 10-fold serial dilutions onto SC-his plates without (-) and with (+) 10 mM 3AT and incubated at indicated temperatures for 3 days. (C) eIF4G2 mutations impair mRNA recruitment to the 40S subunit *in vitro*. Cell-free translation mixture with ^{32}P-labeled poly(A)-tailed *MFA2* mRNA was fractionated by sucrose gradient velocity sedimentation. ^{32}P counts in

relevant fractions are shown with an arrow indicating the fraction containing free 40S subunit. (D) Effect of *tif4632-7R* on *GCN4-lacZ* expression from p180. Graph summarizes β-galactosidase activity of YAS1955 (WT) and KAY901 (*tif4632-7R,* 7R) transformants carrying p180 in the presence (+) or absence (-) of 10 mM 3AT. p value for difference between the values in columns 1 and 3 is presented.

Figure 3

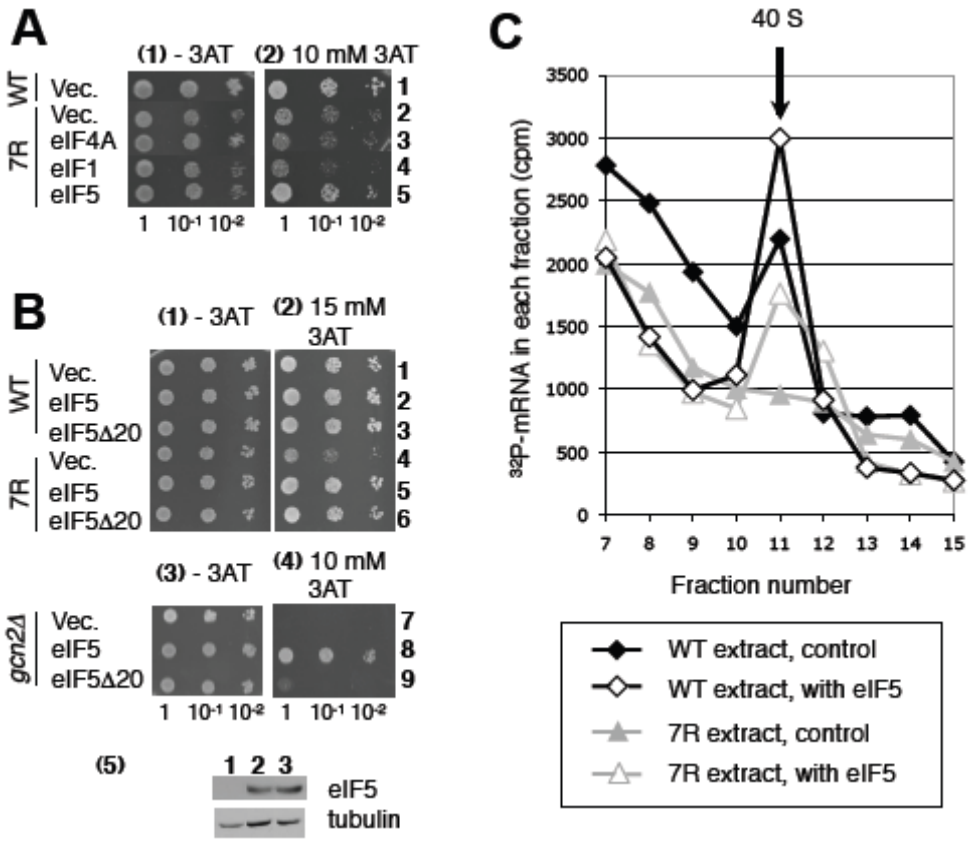

Fig. 3. The interaction of eIF4G2-RS1 with eIF5 mediates mRNA recruitment to the 43S complex. (A, B) Transformants bearing indicated mutations (WT, YAS1955; 7R, KAY874; *gcn2Δ*, KAY24) were diluted and spotted onto SC-his plates without (-3AT) or with (+3AT) the indicated concentrations of 3AT, and the plates were incubated for 3

days (-3AT) and 5 days (+3AT), respectively. In (B), panel 5, shown are immunoblots of 5 μg whole cell extracts from KAY24 transformants (rows 7-9) with antibodies against proteins labeled to the right. (C) eIF4G interaction with eIF5 promotes mRNA recruitment to 40S subunit *in-vitro*. Cell-free translation extracts prepared from strains with indicated mutations (lower box) were incubated with ^{32}P-labeled poly(A)-tailed *MFA2* mRNA with or without FLAG-eIF5 and fractionated by sucrose gradient velocity sedimentation. The assay was analyzed and presented as in Fig. 2E, except the reaction volume was 200 μl and 80 μg of eIF5 was added.

Figure 4

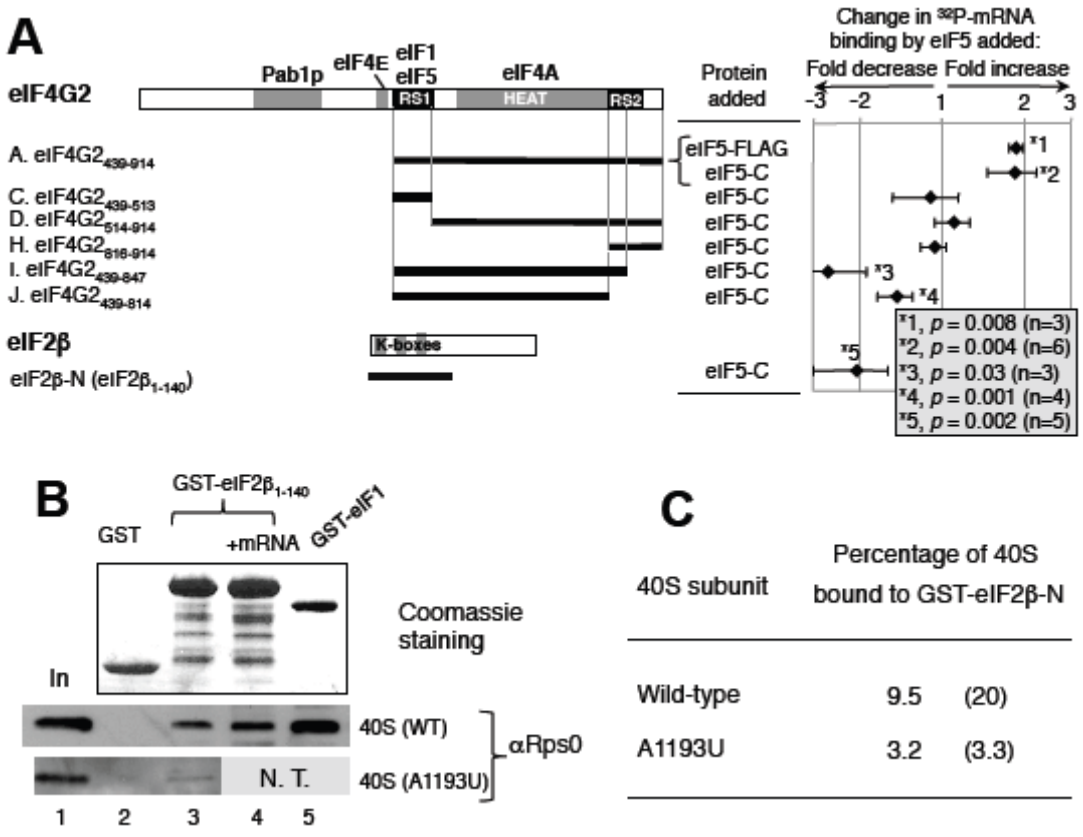

Fig. 4. eIF5 regulates mRNA-binding by eIF4G2 and eIF2β *in vitro*. (A) Primary structure of eIF4G2 with defined binding sites for the indicated initiation factors. Thick lines below represent the portion of eIF4G2 polypeptide found in each construct See Fig. S3 for experimental design. Right panel summarizes fold change in the mRNA binding caused by eIF5 in a logarithmic scale, with their *p* values listed in the box to the right. Positive value indicates fold increase, while negative value indicates fold decrease. Bars indicate SD. GST-eIF2β–N was also tested, as shown at the bottom. (B) Interaction of eIF2β-NTT with the 40S subunit. GST (5 μg), GST-eIF2β-N (10 μg), and GST-eIF1 (5 μg) were bound to the 40S subunit purified from wild-type (WT) or A1193U strain with (+mRNA) or without (blank) non-radiolabeled β-globin mRNA (10 μg). The 40S subunit bound was detected by anti-Rps0 antibodies (bottom gels). Top gel, Coomassie staining of proteins used in this study. In, 25% in-put amount of the 40S subunit. N. T., not tested; however the same preparation of the mutant 40S subunit used here did not bind to GST-eIF1 in a different experiment (29). (C) Summary of percentage of the 40S subunit bound to GST-eIF2β-N calculated from lanes 1 and 3 in (B). Parenthesis indicates values from an independent experiment.

Figure 5

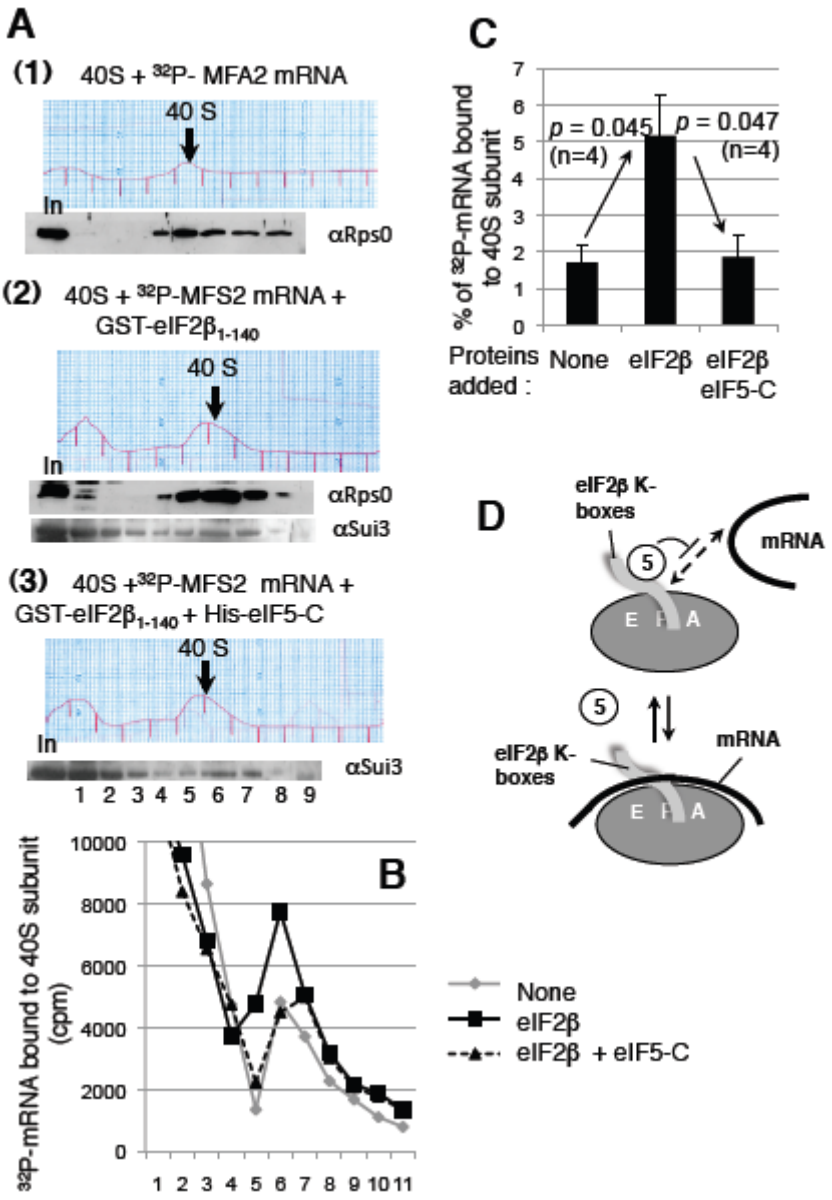

Fig. 5. eIF5-CTD inhibits eIF2β-mediated ^{32}P-MFA2 mRNA binding to the 40S subunit *in vitro*. (A) Purified wild type 40S subunit was incubated in the reaction buffer at 4^{o} C for 90 min with ^{32}P-MFA2 mRNA in the absence (panel 1) and presence of GST-

eIF2β-N (panel 2) or of GST-eIF2β-N and eIF5-C (panel 3). The binding reaction was terminated by crosslinking with formaldehyde (5 min on ice) followed by glycine treatment and fractionated by sucrose gradient velocity sedimentation; A_{254} profile of gradient fractions is shown. The relevant 40S subunit containing fractions are shown with thick arrow, and proteins from one-half of the gradient samples were precipitated by ethanol followed by immunoblot analysis with antibodies raised against proteins listed to the right. In, 10% in-put amount. The resulting immunoblot patterns were shown under corresponding A_{254} profile. (B) Graph shows the scintillation count of the ^{32}P-MFA2 mRNA present in the other half of the gradient samples from the experiments shown in (A). Gray line, panel 1; black straight line, panel 2; black dotted line, panel 3. (C) Graph indicates the amount of ^{32}P-MFA2 mRNA found in 40S subunit fractions in the absence or presence of GST-eIF2β-N (eIF2β) or GST-eIF2β-N and eIF5-CTD (eIF2β eIF5-C). Bars indicate standard errors. (D) Model showing that eIF5-C (empty oval) competes with mRNA (thick line) binding without impeding eIF2β K-box (gray tube) binding to the 40S subunit (gray oval with E, P, A denoting the decoding site).

Figure 6

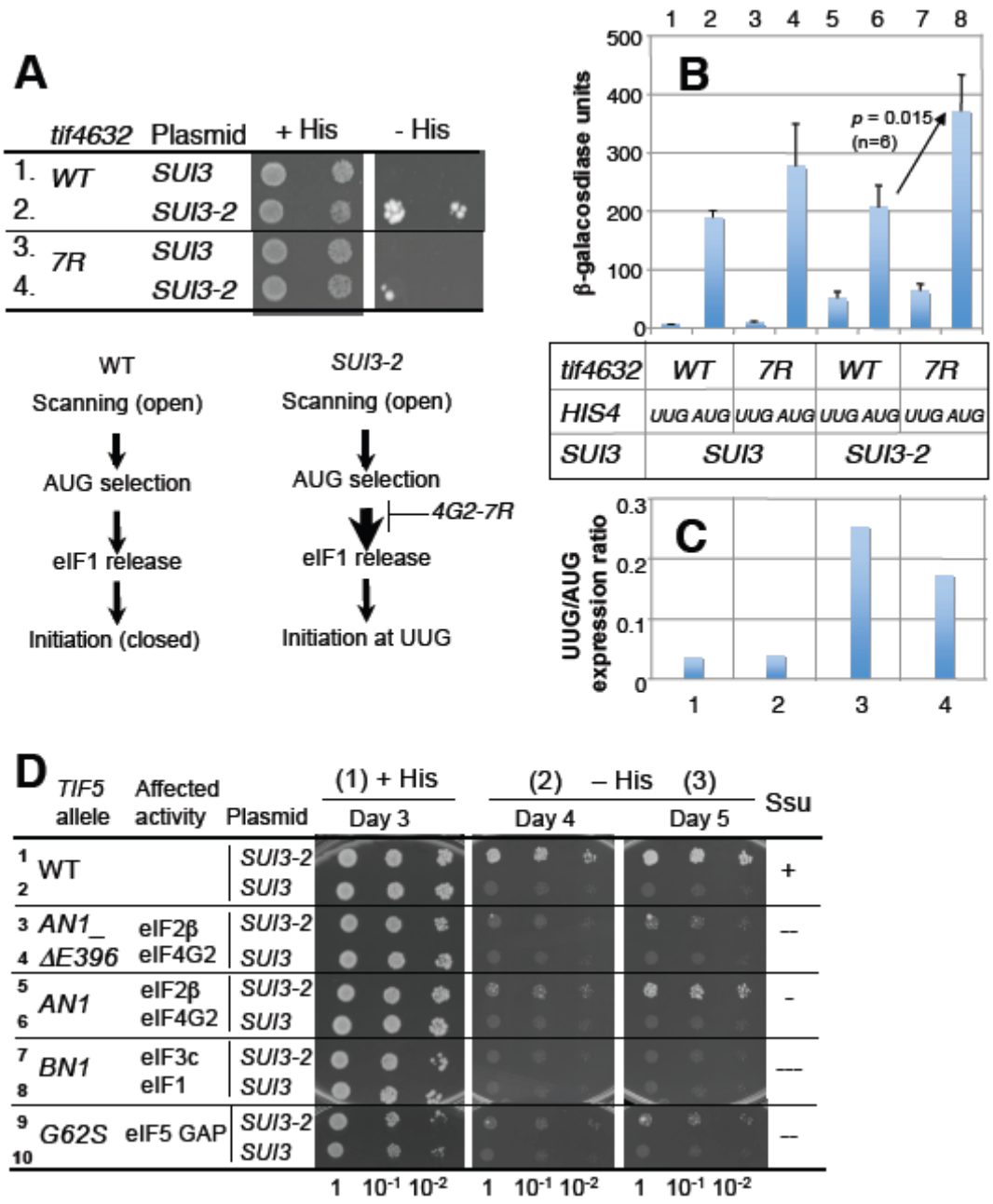

Fig. 6. Mutations in eIF4G2-RS1 and eIF5-CTD suppress relaxed start codon selection caused by eIF2β mutation (*SUI3-2*). (A) 5μl of 0.15 and 0.015 A_{600} unit cultures of transformants of KAY220 (WT) and KAY862 (7R) carrying *SUI3* or *SUI3-2*

URA3 plasmids (Table S1) were spotted onto SC-ura (+*His*) and SC-ura-his (-*His*) plates and incubated at 30^{o} C for 3 and 7 days, respectively. (B) Translation initiation from UUG codons in *tif4632-7R*. Double transformants of YAS1955 (WT) and KAY901 (7R) with a *HIS4-lacZ* reporter plasmid, p367 with its natural start codon, *HIS4*^{AUG}*-lacZ,* or p400 with *HIS4*^{UUG}*-lacZ*, and with *SUI3* or *SUI3-2 ADE2* plasmids (Table S1) were grown in SC-ura-ade medium and assayed for β-galactosidase activity. Shown are the averages and standard errors from 6 independent measurements. (C) Bars indicate the percentage of the *HIS4*^{UUG}*-lacZ* values relative to *HIS4*^{AUG}*-lacZ* values in panel B, calculated as UUG suppression activity. (D) 5μl of 0.15 A_{600} unit culture and its 10-fold serial dilutions of transformants of KAY976 (WT) and its *tif5* derivatives were assayed as in (A) except +His and –His plates were incubated for times indicated above.

Figure 7

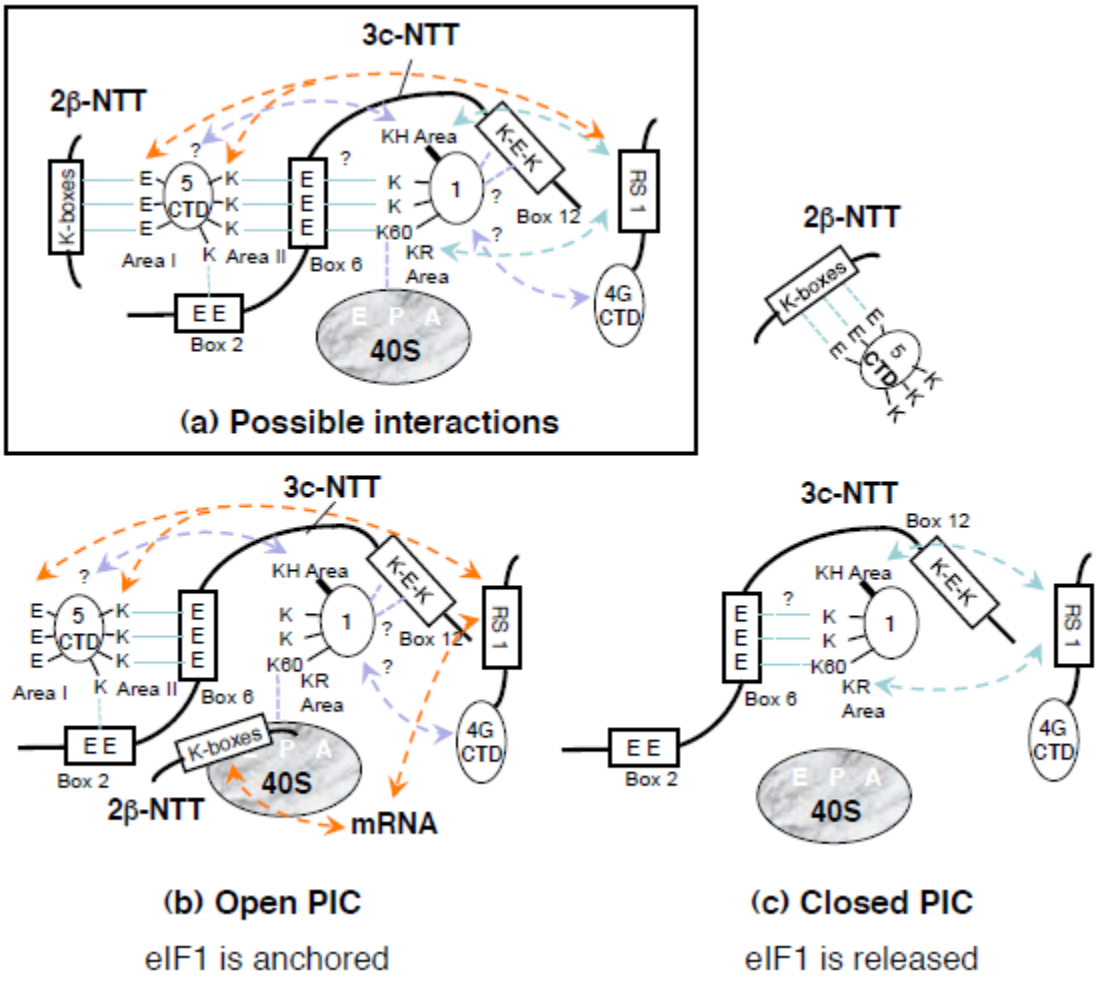

Fig. 7. Hypothetical model of eIF assembly rearrangement within the PIC. (a) Summary of interaction between eIF1 (1), eIF2β-NTT (2β-NTT), eIF3c-NTT (3c-NTT), eIF5-CTD (5-CTD), and eIF4G-CTD (4G-CTD), as well as that between eIF1 (with K60, the ribosome contact site) and the 40S subunit (gray oval with P E A denoting the decoding site). Boxes indicate unstructured charged segments, K-boxes in eIF2β, RS1 in eIF4G and glutamate (E) and lysine (K)-rich segments (boxes 2, 6 and 12) in eIF3c. Circles indicate the folded domains of these eIFs, with charged amino acids (E or K) in

designated surface areas. Dotted line or arrow indicates proposed interaction between the indicated amino acids or surface area (?, interaction surface has not been determined). Orange line, interaction important for mRNA recruitment to or stabilization within the PIC identified in this study. Purple line, mutational disruption of this interaction causes Sui$^-$ phenotype (10, 14, 24, 34, 43). Light blue line, mutational disruption of this interaction causes Ssu$^-$ phenotype (this study) (20, 24, 43). (b and c) The network of interactions stabilizing the open and closed states of the PIC, respectively. The interactions whose mutations cause Sui$^-$ phenotype are proposed to assist anchoring eIF1 to the 40S subunit in (b). The interactions whose mutations cause Ssu$^-$ phenotype (except for eIF5-eIF3c interactions – see text) are proposed to promote eIF1 release in (c).